

Exploring Self-Attention for Visual Intersection Classification

Haruki Nakata, Kanji Tanaka, and Koji Takeda

Abstract—In robot vision, self-attention has recently emerged as a technique for capturing non-local contexts. In this study, we introduced a self-attention mechanism into the intersection recognition system as a method to capture the non-local contexts behind the scenes. An intersection classification system comprises two distinctive modules: (a) a first-person vision (FPV) module, which uses a short egocentric view sequence as the intersection is passed, and (b) a third-person vision (TPV) module, which uses a single view immediately before entering the intersection. The self-attention mechanism is effective in the TPV module because most parts of the local pattern (e.g., road edges, buildings, and sky) are similar to each other, and thus the use of a non-local context (e.g., the angle between two diagonal corners around an intersection) would be effective. This study makes three major contributions. First, we proposed a self-attention-based approach for intersection classification using TPVs. Second, we presented a practical system in which a self-attention-based TPV module is combined with an FPV module to improve the overall recognition performance. Finally, experiments using the public KITTI dataset show that the above self-attention-based system outperforms conventional recognition based on local patterns and recognition based on convolution operations.

I. INTRODUCTION

In the existing scene recognition technology for autonomous driving applications, the convolution operator [1] is often used to process local neighbor information using a fixed weight kernel to hierarchically aggregate the global context. However, this method makes it difficult to capture non-local contexts at a high spatial resolution, which is not sufficient for typical applications where a high inter-class similarity of local feature distributions is expected.

Self-attention [2] has recently emerged as a technique for capturing non-local contexts. An important concept of self-attention is to calculate the global context for a target region as a weighted sum of features over all image regions. The corresponding weights were dynamically calculated using the similarity function between the features of the embedded space at these locations. The number of parameters was independent of the scale at which self-attention handles long-distance interactions. This allowed us to capture non-local contexts with high spatial resolution.

In this study, we introduced a self-attention mechanism into the intersection recognition system as a method to capture the non-local contexts behind the scenes (Fig. 1a). The goal of intersection classification is to classify traffic scenes with respect to the road topology (e.g., a seven-class problem, as illustrated in Fig. 1b). An intersection

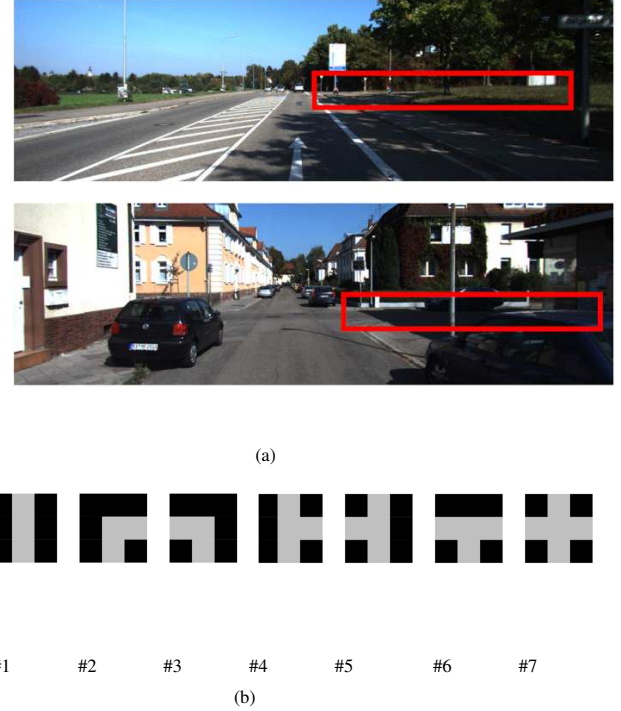


Fig. 1. We aim to exploit the self-attention mechanism within the TPV module in the intersection classification system. (a) Motivative examples: Since most parts of the local pattern (e.g., road edges, buildings, and sky) are similar to each other, the ability of self-attention that can capture non-local context (e.g., the angle between two diagonal corners around an intersection) would be effective). (b) The 7-class intersection classification problem, in which each class corresponds to #1 go straight, #2 turn right, #3 turn left, #4 right facing T-junction, #5 left facing T-junction, #6 bottom facing T-junction, and #7 crossroad as shown in the figures.

classification system consists of two distinctive modules: (a) first-person vision (FPV), which uses a short egocentric view sequence as the intersection is passed; and (b) third-person vision (TPV), which uses a single view immediately before entering the intersection. The self-attention mechanism is effective in the TPV module because most parts of the local pattern (e.g., road edges, buildings, sky) are similar to each other, as shown in Fig. 5; thus, the use of a non-local context (e.g., the angle between two diagonal corners around an intersection) would be effective. Our idea was to exploit self-attention as an end-to-end learning method to capture long-distance contextual information.

This study makes three major contributions. First, we propose a self-attention-based approach for intersection classification using TPVs. Second, we present a practical system in which a self-attention-based TPV module is combined with an FPV module to improve the overall recognition

Our work has been supported in part by JSPS KAKENHI Grant-in-Aid for Scientific Research (C) 17K00361 and 20K12008.

*H. Nakata, K. Tanaka, and K. Takeda are with Department of Engineering, University of Fukui, Japan. tnkknj@u-fukui.ac.jp

performance. Finally, experiments using the public KITTI dataset show that the above self-attention-based system outperforms conventional recognition based on local patterns and recognition based on convolution operations.

II. RELATED WORK

Intersection recognition is formulated as an image-classification problem. For example, [3] presented an approach based on a cascade of feature extractors and classification modules. More recently, deep learning approaches, such as the application of a deep convolutional neural network to this problem, have proven to be effective by several researchers. For example, [4] presented a multitask learning method that simultaneously performs intersection recognition and segmentation tasks. Other traffic scene recognition problems have also been studied extensively. For example, crossability prediction [5] and the division/reconstruction of crossable road areas [6]. In [7], a deep convolutional neural network-based road surface classifier was employed to distinguish between six road surface types. In [8], a data-adaptive similarity scale was used to cluster the traffic conditions. In [9], a large-scale input image was used for crack detection. In [6], a monocular detection method was proposed for robust road detection under severe occlusions. In [10], contextual information and traffic rules were considered to predict pedestrian movement. In [11], a stereo vision algorithm was used to estimate the scene layout by describing static/dynamic objects. In [12], this study was extended to detect intersections in a view-invariant manner.

Intersection recognition is closely related to the problem of road topology recognition based on ego-motion predictions. In [13], map-based self-localization was achieved using the motion cues of a vehicle measured by visual odometry. In [14], a visual odometry method was developed to calculate the movement of a monocular camera with six degrees of freedom, assuming that the ground plane is known. In [15], a robust new visual odometry framework was presented by considering the motion model of the vehicle. In [16], an end-to-end deep learning framework was used to train a regressor for visual odometry. In [17], a hierarchical graph-based scene representation was used to understand complex urban environments. Other video-analysis problems have also been studied extensively. For example, in [18], lane change prediction was studied using LSTM. In [19], the performance of a lateral-position prediction algorithm was evaluated. In [20], a situation resulting from future lane changes was predicted. In [21], a probabilistic multisession framework was developed using high-precision road maps for urban areas using low-cost sensors. In [22], intersection detection was studied as a binary classification problem using LSTM based on a monocular sequence. In [23], a framework was developed for the simultaneous estimation of highway traffic conditions and traffic flow parameters.

Studies have also been conducted with additional cues from other modalities, such as global positioning systems (GPS) [24], publicly available map data [25], road signs [26], and domain-specific prior knowledge, such as traffic lights

[27]. Recent research examples include the classification and interpretation of signs that are not affected by the weather [28], detection of traffic lights and small objects [29], detection and recognition of signs [26], hierarchical detection of traffic lights [30], and cross-dataset classification of traffic lights [31]. In addition, detecting and tracking moving objects and pedestrians to predict the road area where the vehicle can travel contributes to intersection recognition from another direction [32].

The proposed approach has three main advantages. First, to the best of our knowledge, we are the first to explore the self-attention approach in the context of visual intersection classification. Second, our framework achieves improved performance by combining the above self-attention-based TPV with the FPV approach for ego-motion prediction. Third, this framework consists of a minimal set of modules, FPV and TPV, which are complementary and orthogonal to the aforementioned methods based on other modalities.

III. PROPOSED APPROACH

We aim to boost the intersection classification system, which consists of FPV and TPV modules, by introducing a self-attention mechanism to capture the global context. Figure 2 presents an overview of the proposed framework. Specifically, the self-attention mechanism was applied to the TPV module (“T-Net” in Fig. 2), in which the 7-class intersection classification problem was directly addressed (Section III-A). Subsequently, the FPV module (“F-Net” in Fig. 2) is introduced as a motion classifier. It classifies vehicle ego-motions into three major classes: “go straight,” “turn right,” and “turn left”. Thereafter, the FPV module is combined with the TPV module to improve the overall performance of intersection classification (Section III-B). The output of either the FPV or TPV module is in the form of a class-specific probability density vector (PDV). Although the FPV module is implemented in the proposed method as a 3-class motion classifier, it can be implemented to address the 7-class intersection classification directly, which will be discussed in an ablation study in the experimental section (Section IV).

A. Self-attention Mechanism

The self-attention mechanism was originally revolutionized extensively in areas, such as natural-language processing and machine translation. Since then, it has been applied in fields, such as image recognition, question answering, and image generation [33]. However, until recently, it has been used to complement the convolution operations, adjust the output of the convolution, or create a layer that is used by combining the convolution with other methods. However, recent studies have shown that limiting self-attention to local patches can adapt it to the network and create better models in terms of robustness and generalization [2].

In [2], a method of using an image recognition model with a self-attention mechanism was proposed as a study of scene classification. It addresses two variants: patch-wise and pairwise self-attention. The patch-wise method

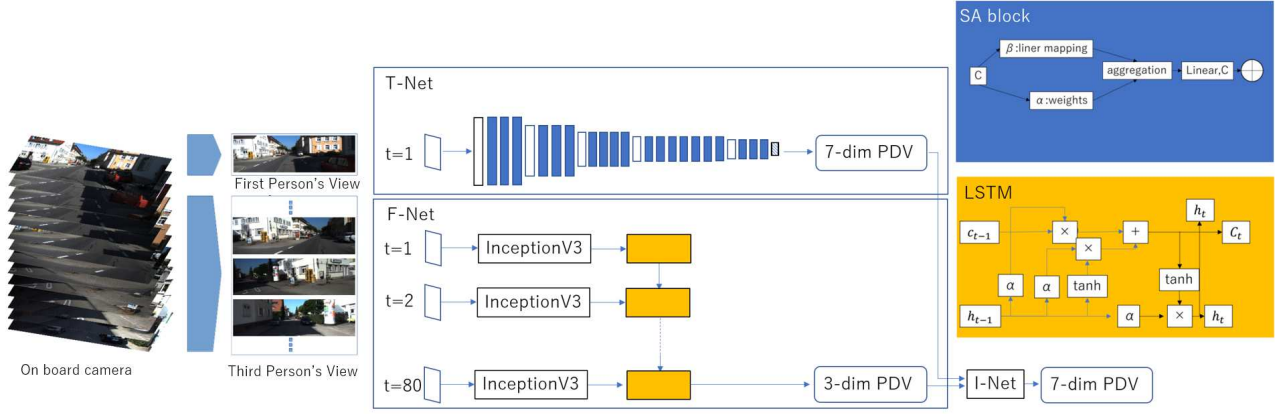


Fig. 2. System overview.

can uniquely identify a particular location in a footprint. Pairwise generalizes the self-attention mechanism to standard dot product attention. In our implementation, patch-wise self-attention showed a higher performance empirically, and we decided to use it as the default method. In this case, self-attention takes the form

$$y_i = \sum_{j \in R(i)} \alpha(x_{R(i)})_j \odot \beta(x_j), \quad (1)$$

where $x_{R(i)}$ is a patch of the feature vector of footprint $R(i)$, and $\alpha(x_{R(i)})$ is a tensor with the same spatial dimension as the patch $x_{R(i)}$. $\alpha(x_{R(i)})_j$ is the vector at location j in this tensor, and it corresponds to the vector x_j in $x_{R(i)}$. Contrary to a CNN, which can handle only nearby information, in self-attention, the weight calculation $\alpha(x_{R(i)})$ can be indexed individually and the feature vector x_j can be indexed by location. This makes it possible to fuse the feature vector information from different locations in the footprint. $\alpha(x_{R(i)})$ is assumed to be decomposed by the equation:

$$\alpha(x_{R(i)}) = y(\delta(x_{R(i)})). \quad (2)$$

For $\delta(x_{R(i)})$, three different combinations as followings are explored:

- Star-product:

$$\delta(x_{R(i)}) = [\varphi(x_i)^T \psi(x_j)]_{\forall j \in R(i)} \quad (3)$$

- Clique-product:

$$\delta(x_{R(i)}) = [\varphi(x_j)^T \psi(x_k)]_{\forall j, k \in R(i)} \quad (4)$$

- Concatenation:

$$\delta(x_{R(i)}) = [\varphi(x_i), [\psi(x_j)]_{\forall j \in R(i)}] \quad (5)$$

The star product has small flops, but its accuracy is not satisfactory. Concatenation has the highest accuracy among the three types; however, it has large flops. The liquid product had a good balance between the two methods.

In this study, we prioritized accuracy and used concatenation.

We pretrained the self-attention mechanism on ImageNet, a large dataset of 1,000 object classes, and then adapted the model to the target task via transfer learning. The fully connected layer of the final layer is modified into seven classes. Fine-tuning was then performed to adapt to a new task. For fine-tuning, the weights of the six layers, including the fully connected layer and transition layer in the architecture, were set learnable, and those of the other layers were prefixed.

Figure 2 presents an overview of the TPV module (“T-Net”). As shown in the figure, the TPV module comprised five transition layers, 19 self-attention blocks, and one output layer. A CNN was used for feature extraction and conversion.

There are five transition layers, each output is $112 \times 112 \times 64$, $56 \times 56 \times 256$, $28 \times 28 \times 512$, $14 \times 14 \times 1,024$, and $7 \times 7 \times 2,048$. By lowering the spatial resolution, the computational load is reduced and the receptive field is expanded. The transition consists of a batch normalization layer, ReLU [34], 2×2 maximum pooling with stride 2, and a linear mapping that extends the channel dimension.

In the self-attention block (“SA block” in Fig. 2), the input feature tensor (channel dimension C) passes through two processing streams. The stream at the bottom evaluates the attention weight α by computing the function δ (via the mappings φ and ψ) followed by the mapping γ . The stream at the top applies a linear transformation β that transforms the input features and reduces their dimensions for efficient processing. The outputs of the two streams were aggregated using the Hadamard product. The combined features undergo normalization and elementwise nonlinearization and are then processed in the final linear layer, to expand the dimension to C .

B. FPV-TPV Framework

Deep visual odometry in [16] was employed as the basis for our F-Net (“F-Net” in Fig. 2). It combines the advantages of convolutional neural network and recursive LSTM neural network, and is one of the best-known methods for ego-motion estimation.

Using raw sequence images as the input of the LSTM did not yield a good performance experimentally. We found that using an optical flow sequence instead of a raw sequence often significantly improves performance. Therefore, this optical flow-based variant was used in our study. Each pixel of an optical flow image is the intensity and direction calculated from the 2-channel array containing the optical flow vector (u, v) [35], and is then color-coded.

The FPV module processes the features of each frame using LSTM (“LSTM” in Fig. 2). It extracts 2,048-dimensional features from the feature extraction part of the convolutional neural network of Inception V3 for each frame. This feature vector is used as the input for the LSTM for each time step. Thereafter, for the feature extraction part using Inception V3, feature extraction was performed using the weights learned by ImageNet as they were. Subsequently, the parameters of the FPV module were updated by setting only the LSTM and fully connected layer to be learnable.

In this study, the posterior distribution of each class was obtained using the output of the FPV module as a prior distribution and expanding the output of the TPV module (“I-Net” in Fig. 2). The output of the I-Net is calculated as $I[c] = W_S[c]P_M[c]$ for each class c . Furthermore, when the confidence of top-1 of the FPV module is 0.9999 or higher, the 7-dimensional mask vector T is introduced, and $I[c] = W_S[c]P_M[c]T[c]$. W_S assumes one of the three values depending on the results of the FPV module. This is controlled by the ego-motion class c^- ($\in \{ \text{“go straight,” “turn right,” “turn left”} \}$) that received the lowest likelihood value: If c^- is “go straight”:

$$W_S = (0, 1, 1, 1, 1, 1, 1),$$

or if c^- is “turn right”:

$$W_S = (1, 0, 1, 1, 1, 1, 1)$$

or if c^- is “turn left”:

$$W_S = (1, 1, 0, 1, 1, 1, 1)$$

In addition, the mask vector T is controlled by the ego-motion class c^+ ($\in \{ \text{“go straight,” “turn right,” “turn left”} \}$) that received the highest likelihood value: If c^+ is “go straight”:

$$T = (1, 0, 0, 0, 1, 1, 1)$$

or if c^+ is “turn right”:

$$T = (0, 1, 0, 1, 1, 0, 1)$$

or if c^+ is “turn left”:

$$T = (0, 0, 1, 1, 0, 1, 1)$$

IV. EVALUATION EXPERIMENTS

The KITTI dataset was used to experimentally evaluate the proposed method and other comparative methods.



Fig. 3. Examples of views corresponding to [-5, -10] m from the intersection location.

TABLE I
PERFORMANCE RESULTS

method	top-1 accuracy
TPV	0.57
FPV	0.31
VGG16	0.52
SIFT+NBNN	0.16
LCF+NBNN	0.23
AE+L2	0.22
Ours	0.59

A. Comparing Methods

Six comparing methods, TPV, FPV, VGG16, SIFT+NBNN, LCF+NBNN, and AE+L2 were employed for performance comparison. (1) The TPV method uses a T-Net based on the self-attention mechanism, as described in Section III-A. (2) The FPV method is based on almost the same architecture as F-Net, but the output layer is modified to address the 7-class intersection classification directly, not the 3-class motion classification. (3) The VGG16 method is a convolutional neural network consisting of 13 convolutional layers and three fully connected layers, for a total of 16 layers [36]. In its training stage, publicly available weights pretrained on ImageNet were further finetuned to address the 7-class problem. (4) SIFT+NBNN is based on the scene representation of a bag of 128-dim SIFT features [37] with Harris-Laplace keypoints (1,500-2,000 per image) using the naive Bayes nearest neighbor (NBNN) distance metric [38]. (5) LCF+NBNN is different from SIFT+NBNN only in that the 512-dim LCF feature [39] (768 per image) is used instead of the 128-dim SIFT. (6) AE+L2 is based on a global 3,136-dim autoencoder (AE) feature with the nearest neighbor-based distance metric [40]. Our decision to use the NBNN distance metric was motivated by its success in previous studies on visual place recognition [41]. We used L2-norm to measure the distance between a feature pair for all the methods.

B. Settings

In this study, a new dataset was created by extracting the entire intersection image and the intersection passage sequence from the KITTI data set [42]. The image from the left eye of the stereo camera of the KITTI dataset was

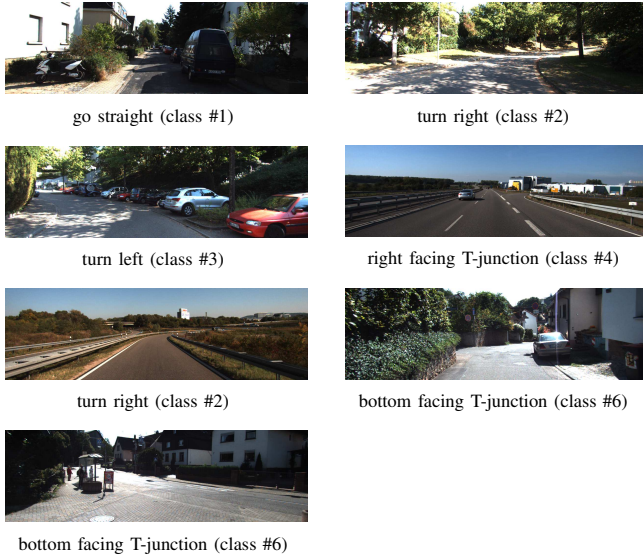


Fig. 4. Examples of input images

used as the input for our system. The image size is 241×376 pixels. The input layer of the T-Net was slightly modified to address our image size of 224×224 pixels. The input images of the FPV module derived from Inception V3 were resized to 299×299 pixels to be fitted to the network. To stabilize the training process, the training sequences for F-Net were clustered in terms of the time interval and clusters whose size is smaller than five were not used for training.

The details of the training are as follows. A GeForce RTX 3090 GPU is used to train the TPV and FPV modules. A PyTorch virtual environment and Keras with a TensorFlow backend were used for the F-Net and I-Net. The number of epochs was set as 20.

The details of dataset creation are as follows. We manually analyzed the GPS information and obtained an image corresponding to the range $[-L_2, -L_1]$ from the center of the intersection. The hyper-parameters are set as $L_1=0$ [m], and $L_2=5$ [m] following [43]. From these images, 152 images were extracted for each of the seven classes. An example of an image of the KITTI dataset corresponding to this interval is shown in Fig. 3. The image set was divided into 126 training datasets and 36 test datasets. The average length of the resulting sequence was approximately 22 m.

Top-1 accuracy was used as a performance index.

The KITTI dataset [42] was obtained from a sensor-equipped vehicle in an urban environment in Karlsruhe, Germany. Formally, Visual Odometry/SLAM Evaluation 2012 in the KITTI dataset was used. An example of an image used is shown in Fig. 4. This dataset consists of 22 stereo sequences, 11 of which have acquired GPS coordinates, and the remaining 11 have no GPS coordinates. The camera uses PointGray Flea2 video cameras. The frame rate is 10 ps. The image resolution was modified from the original setting of $1,392 \times 512$ pixels to that of the KITTI dataset of $1,241 \times 376$ pixels.

C. Results

Table I presents the performance results. The accuracy of the proposed method, which is based on the self-attention mechanism, was higher than that of any comparison method. Notably, ablation consisting of only the TPV module with the self-attention mechanism outperformed the baseline method of VGG16. In the early stages of the experiment, training was performed without using the weights pre-trained on ImageNet, and the accuracy was not high. However, fine-tuning of the weights pretrained on ImageNet significantly improved the accuracy.

Figure 5 shows several success and failure examples for the self-attention-based TPV method. In the first failure example, the image was predicted as “turn right”. This may be because the gray-colored pixels on the right side part of the image were recognized as a road region. Notably, such a failure could be resolved by introducing the FPV module, which significantly improved the discriminativity between right and left turns. For the second example, the ground-truth intersection class was the right facing T-junction (class #4), but in the failure example, it is predicted as a bottom facing T-junction (class #6). This might be because the angle of the road on the left side of the T-junction is close to going straight. For the third example, the ground-truth class was crossroads (class #7), but in the failure example, it was predicted as a right facing T-junction (class #4). In this case, the road on the left was hidden behind a black car, and because of this, it was incorrectly classified right facing T-junction (class #4). What is common to many examples is that the recognition often failed when the viewpoint location is distant from the center of the intersection. Figure 6 shows the statistics of the classification results in the form confusion matrix.

Currently, the I-Net is not trained end-to-end; instead, a handcrafted network is used. Notably, the performance of this handcrafted code is satisfactory in several situations. It often outperformed the machine learning variants we tried during the development process. However, failure modes were also observed. One such failure mode is the case in which the FPV module fails to predict the ego-motion because the rule prioritizes FPV decisions over TPV decisions. In other words, our framework may fail with high confidence. To avoid such a failure, statistics-based methods, such as neural networks or perceptron methods, would be effective and should be explored in future work.

V. CONCLUSIONS

In this study, we addressed the intersection classification problem from the perspective of the self-attention mechanism. This self-attention method was effectively incorporated into the unified FPV-TPV framework. Experiments verified that the self-attention-based TPV module is complementary to the FPV module and can improve the overall performance of the intersection classification.



Fig. 5. Example results of TPV module.

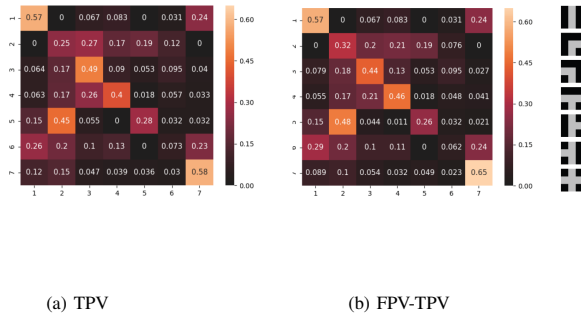


Fig. 6. Confusion matrix.

REFERENCES

- [1] Andreas Ess, Tobias Muller, Helmut Grabner, and Luc Van Gool. Segmentation-based urban traffic scene understanding. In *BMVC*, volume 1, page 2, 2009.
- [2] Hengshuang Zhao, Jiaya Jia, and Vladlen Koltun. Exploring self-attention for image recognition. In *Proceedings of the IEEE/CVF Conference on Computer Vision and Pattern Recognition*, pages 10076–10085, 2020.
- [3] Malte Oeljeklaus, Frank Hoffmann, and Torsten Bertram. A combined recognition and segmentation model for urban traffic scene understanding. In *2017 IEEE 20th International Conference on Intelligent Transportation Systems (ITSC)*, pages 1–6, 2017.
- [4] Malte Oeljeklaus, Frank Hoffmann, and Torsten Bertram. A combined recognition and segmentation model for urban traffic scene understanding. In *2017 IEEE 20th International Conference on Intelligent Transportation Systems (ITSC)*, pages 1–6, 2017.
- [5] Charles Richter, William Vega-Brown, and Nicholas Roy. Bayesian learning for safe high-speed navigation in unknown environments. In *Robotics Research*, pages 325–341. Springer, 2018.
- [6] Tarlan Suleymanov, Paul Amayo, and Paul Newman. Inferring road boundaries through and despite traffic. In *2018 21st International Conference on Intelligent Transportation Systems (ITSC)*, pages 409–416, 2018.
- [7] Marcus Nolte, Nikita Kister, and Markus Maurer. Assessment of deep convolutional neural networks for road surface classification. In *2018 21st International Conference on Intelligent Transportation Systems (ITSC)*, pages 381–386, 2018.
- [8] Friedrich Kruber, Jonas Wurst, and Michael Botsch. An unsupervised random forest clustering technique for automatic traffic scenario categorization. In *2018 21st International Conference on Intelligent Transportation Systems (ITSC)*, pages 2811–2818, 2018.
- [9] Kaige Zhang, Heng-Da Cheng, and Shan Gai. Efficient dense-dilation network for pavement cracks detection with large input image size. In *2018 21st International Conference on Intelligent Transportation Systems (ITSC)*, pages 884–889, 2018.
- [10] Markus Koschi, Christian Pek, Mona Beikirch, and Matthias Althoff. Set-based prediction of pedestrians in urban environments considering formalized traffic rules. In *2018 21st international conference on intelligent transportation systems (ITSC)*, pages 2704–2711, 2018.
- [11] Andreas Geiger, Martin Lauer, Christian Wojek, Christoph Stiller, and Raquel Urtasun. 3d traffic scene understanding from movable platforms. *IEEE transactions on pattern analysis and machine intelligence*, 36(5):1012–1025, 2013.
- [12] Abhijeet Kumar, Gunshi Gupta, Avinash Sharma, and K Madhava Krishna. Towards view-invariant intersection recognition from videos using deep network ensembles. In *2018 IEEE/RSJ International Conference on Intelligent Robots and Systems (IROS)*, pages 1053–1060, 2018.
- [13] Marcus A Brubaker, Andreas Geiger, and Raquel Urtasun. Map-based probabilistic visual self-localization. *IEEE transactions on pattern analysis and machine intelligence*, 38(4):652–665, 2015.
- [14] Andreas Geiger, Julius Ziegler, and Christoph Stiller. Stereoscan: Dense 3d reconstruction in real-time. In *2011 IEEE intelligent vehicles symposium (IV)*, pages 963–968, 2011.
- [15] Johannes Graeter, Tobias Strauss, and Martin Lauer. Momo: Monocular motion estimation on manifolds. In *2017 IEEE 20th International Conference on Intelligent Transportation Systems (ITSC)*, pages 1–6, 2017.
- [16] Sen Wang, Ronald Clark, Hongkai Wen, and Niki Trigoni. Deepvo: Towards end-to-end visual odometry with deep recurrent convolutional

- neural networks. In *2017 IEEE international conference on robotics and automation (ICRA)*, pages 2043–2050, 2017.
- [17] Lars Kunze, Tom Bruls, Tarlan Suleymanov, and Paul Newman. Reading between the lanes: Road layout reconstruction from partially segmented scenes. In *2018 21st International Conference on Intelligent Transportation Systems (ITSC)*, pages 401–408. IEEE, 2018.
- [18] Hien Q Dang, Johannes Fürnkranz, Alexander Biedermann, and Maximilian Hoepfl. Time-to-lane-change prediction with deep learning. In *2017 IEEE 20th International Conference on Intelligent Transportation Systems (ITSC)*, pages 1–7, 2017.
- [19] Ruben Izquierdo, Ignacio Parra, Jesús Muñoz-Bulnes, D Fernández-Llorca, and MA Sotelo. Vehicle trajectory and lane change prediction using ann and svm classifiers. In *2017 IEEE 20th International Conference on Intelligent Transportation Systems (ITSC)*, pages 1–6, 2017.
- [20] Veit Leonhardt and Gerd Wanielik. Feature evaluation for lane change prediction based on driving situation and driver behavior. In *2017 20th International Conference on Information Fusion (Fusion)*, pages 1–7, 2017.
- [21] Stefan Boschenriedter, Phillip Hossbach, Clemens Linnhoff, Stefan Luthardt, and Siqian Wu. Multi-session visual roadway mapping. In *2018 21st International Conference on Intelligent Transportation Systems (ITSC)*, pages 394–400, 2018.
- [22] Dhaivat Bhatt, Danish Sodhi, Arghya Pal, Vineeth Balasubramanian, and Madhava Krishna. Have i reached the intersection: A deep learning-based approach for intersection detection from monocular cameras. In *2017 IEEE/RSJ International Conference on Intelligent Robots and Systems (IROS)*, pages 4495–4500, 2017.
- [23] Yue Zhou, Edward Chung, Michael E Cholette, and Ashish Bhaskar. Real-time joint estimation of traffic states and parameters using cell transmission model and considering capacity drop. In *2018 21st International Conference on Intelligent Transportation Systems (ITSC)*, pages 2797–2804, 2018.
- [24] Y Byon, Amer Shalaby, and Baher Abdulhai. Travel time collection and traffic monitoring via gps technologies. In *2006 IEEE Intelligent Transportation Systems Conference*, pages 677–682, 2006.
- [25] Benedict Flade, Marcos Nieto, Gorka Velez, and Julian Eggert. Lane detection based camera to map alignment using open-source map data. In *2018 21st International Conference on Intelligent Transportation Systems (ITSC)*, pages 890–897, 2018.
- [26] Any Gupta and Ayesha Choudhary. A framework for real-time traffic sign detection and recognition using grassmann manifolds. In *2018 21st International Conference on Intelligent Transportation Systems (ITSC)*, pages 274–279, 2018.
- [27] Martin Bach, Daniel Stumper, and Klaus Dietmayer. Deep convolutional traffic light recognition for automated driving. In *2018 21st International Conference on Intelligent Transportation Systems (ITSC)*, pages 851–858, 2018.
- [28] Paul Amayo, Tom Bruls, and Paul Newman. Semantic classification of road markings from geometric primitives. In *2018 21st International Conference on Intelligent Transportation Systems (ITSC)*, pages 387–393, 2018.
- [29] Julian Müller and Klaus Dietmayer. Detecting traffic lights by single shot detection. In *2018 21st International Conference on Intelligent Transportation Systems (ITSC)*, pages 266–273, 2018.
- [30] Michael Weber, Matthias Huber, and J Marius Zöllner. Hdtr: A cnn based hierarchical detector for traffic lights. In *2018 21st International Conference on Intelligent Transportation Systems (ITSC)*, pages 255–260, 2018.
- [31] Carlos Fernández, Carlos Guindel, Niels-Ole Salscheider, and Christoph Stiller. A deep analysis of the existing datasets for traffic light state recognition. In *2018 21st International Conference on Intelligent Transportation Systems (ITSC)*, pages 248–254, 2018.
- [32] MS Suraj, Hugo Grimmer, Lukáš Platinský, and Peter Ondruška. Predicting trajectories of vehicles using large-scale motion priors. In *2018 IEEE Intelligent Vehicles Symposium (IV)*, pages 1639–1644, 2018.
- [33] Zhilin Yang, Zihang Dai, Yiming Yang, Jaime Carbonell, Russ R Salakhutdinov, and Quoc V Le. Xlnet: Generalized autoregressive pretraining for language understanding. *Advances in neural information processing systems*, 32, 2019.
- [34] Vinod Nair and Geoffrey E Hinton. Rectified linear units improve restricted boltzmann machines. In *Icml*, 2010.
- [35] Gunnar Farnéback. Two-frame motion estimation based on polynomial expansion. In *Scandinavian conference on Image analysis*, pages 363–370. Springer, 2003.
- [36] Karen Simonyan and Andrew Zisserman. Very deep convolutional networks for large-scale image recognition. *arXiv preprint arXiv:1409.1556*, 2014.
- [37] David G Lowe. Object recognition from local scale-invariant features. In *Proceedings of the seventh IEEE international conference on computer vision*, volume 2, pages 1150–1157. Ieee, 1999.
- [38] Tatiana Tommasi and Barbara Caputo. Frustratingly easy nbnn domain adaptation. In *Proceedings of the IEEE International Conference on Computer Vision*, pages 897–904, 2013.
- [39] Sugimoto Takuma, Tanaka Kanji, and Yamaguchi Kousuke. Leveraging object proposals for object-level change detection. In *2018 IEEE Intelligent Vehicles Symposium (IV)*, pages 397–402. IEEE, 2018.
- [40] Oren Boiman, Eli Shechtman, and Michal Irani. In defense of nearest-neighbor based image classification. In *2008 IEEE conference on computer vision and pattern recognition*, pages 1–8. IEEE, 2008.
- [41] Tanaka Kanji. Self-localization from images with small overlap. In *2016 IEEE/RSJ International Conference on Intelligent Robots and Systems (IROS)*, pages 4497–4504. IEEE, 2016.
- [42] Andreas Geiger, Philip Lenz, and Raquel Urtasun. Are we ready for autonomous driving? the kitti vision benchmark suite. In *2012 IEEE conference on computer vision and pattern recognition*, pages 3354–3361. IEEE, 2012.
- [43] Koji Takeda and Kanji Tanaka. Use of first and third person views for deep intersection classification. *CoRR*, abs/1901.07446, 2019.